Aggregation and Water-Membrane Partition as Major Determinants of the Activity of the Antibiotic Peptide Trichogin GA IV

Lorenzo Stella,* Claudia Mazzuca,* Mariano Venanzi,* Antonio Palleschi,* Mara Didonè,[†] Fernando Formaggio,[†] Claudio Toniolo,[†] and Basilio Pispisa*

*Dipartimento di Scienze e Tecnologie Chimiche, Università di Roma Tor Vergata, 00133 Rome, Italy; and [†]Istituto di Chimica Biomolecolare, Consiglio Nazionale delle Ricerche, Dipartimento di Chimica Organica, Università di Padova, 35131 Padua, Italy

ABSTRACT   Water-membrane partition and aggregation behavior are fundamental aspects of the biological activity of antibiotic peptides, natural compounds causing the death of pathogenic organisms by perturbing the permeability of their membranes. A synthetic fluorescent analog of the natural lipopeptaibol trichogin GA IV was used to study its interaction with model membranes. Time-resolved fluorescence data show that in water, an equilibrium between monomers and small aggregates is present, the two species having different affinity for membranes. Therefore, association curves are strongly dependent on peptide concentration. A similar heterogeneity is present in the membrane phase, which strongly suggests the occurrence of a monomer-aggregate equilibrium in this case, too. The relative population of each species was determined and a strong correlation between the concentration of membrane-bound aggregates and membrane leakage was found, thereby suggesting that liposome perturbation is due to peptide aggregates only. Light-scattering measurements demonstrate that leakage is not due to liposome micellization. Moreover, experiments with markers of different sizes show that molecules with a diameter of ~4 nm are released only to a minor extent. Overall, these results suggest that, within the concentration range explored, pore formation by peptide aggregates is the most likely mechanism of action for trichogin in membranes.

INTRODUCTION

Antibiotic peptides constitute a major component of the innate defense system shared by organisms from throughout the phylogenetic tree, including humans (Epand and Vogel, 1999). In higher organisms, they complement the highly specific, antibody-mediated antigen recognition, a relatively slow process, by acting shortly after microbial infection and being effective against a wide range of microbes, including bacteria, fungi, and protozoa. Their main mechanism of action is the alteration of the permeability of cell membranes, leading to cell death by collapse of transmembrane electro-chemical gradients and osmolysis; this process usually does not involve any specific receptor, as shown by the fact that enantiomers of lytic peptides, composed solely by D-amino acids, maintain a biological activity comparable to that of parent molecules, and by the parallelism generally found between antibiotic activity and the ability to alter the permeability of model membranes (Shai, 2002). For these reasons, antibiotic peptides are the subject of intense research aimed at the creation of a new class of anti-infective therapeutics, to address the rapidly growing problem of pathogenic organisms that are multi-resistant to traditional antimicrobial agents (Zasloff, 2002).

Notwithstanding the large number of studies published in this area, the molecular details of the mechanism by which antibiotic peptides alter the permeability of membranes are still debated and several models have been proposed (Epand and Vogel, 1999; Matsuzaki, 2001, Yang et al., 2001). However, it is evident that the affinity for membranes and the ability to self-associate both in the membrane and water phases are of paramount importance for the definition of the specific mechanism followed by an antibiotic peptide to induce membrane permeability. Cationic peptides can easily bind to the membrane surface, but their insertion in the hydrophobic core of the phospholipid bilayer or their aggregation would be very unfavorable due to their charge. Therefore, their mechanism of action is probably better described by the Shai-Matsuzaki-Huang model (also called "carpet" or "toroidal pore" model), in which peptides bind in a carpet-like arrangement to the membrane surface, inserting in the polar headgroups region. This creates an unfavorable elastic tension that results in the formation of transient defects or pores (Chen et al., 2002). On the other hand, highly hydrophobic peptides that do not include in their sequence many charged amino acids can follow the "barrel stave" model, in which several peptide chains aggregate in a transmembrane orientation to form a well-defined channel. These two classes of peptides are also expected to show a different spectrum of activities: cationic peptides bind much more favorably to membranes formed by anionic lipids (such as those of bacteria) than to zwitterionic bilayers (as in mammal or fungal cells), and therefore usually are much more selective. The binding of hydrophobic peptides, on the other hand, is driven by hydrophobic rather than electrostatic interactions, and therefore these systems often possess also a very interesting fungicidal activity (Shai, 2002). The two classes of peptides are expected to differ also

in their behavior in water, since hydrophobic peptides are much more likely to form aggregates in this phase.

In this article we address these points, by taking trichogin GA IV as an example. This natural peptide, extracted from the soil fungus *Trichoderma longibrachiatum* (Auvin-Guette et al., 1992), has the following amino acid sequence:

$$\text{Oct-Aib}^1\text{-Gly}^2\text{-Leu}^3\text{-Aib}^4\text{-}$$

$$\text{Gly}^5\text{-Gly}^6\text{-Leu}^7\text{-Aib}^8\text{-Gly}^9\text{-Ile}^{10}\text{-Lol},$$
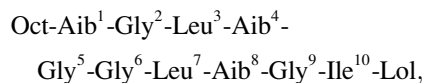
where Oct is *n*-octanoyl, and Lol is leucinol. Trichogin GA IV is the main component of the lipopeptaibol family (Toniolo et al., 2001), formed by linear peptides characterized by a fatty acyl moiety at the N-terminus, a C-terminal 1,2-amino alcohol, and the presence of the $C^{\alpha,\alpha}$-disubstituted glycine Aib (α-aminoisobutyric acid), a helix inducing residue (Karle and Balaram, 1990; Pispisa et al., 2000a,b). Indeed, structural studies in solution and in membrane-mimetic environments have shown that trichogin is significantly structured, populating helical conformations (Auvin-Guette et al., 1992; Toniolo et al., 1994, 1996, 2001). Tric-OMe, a synthetic trichogin analog with a leucine methyl ester at the C-terminus replacing Lol, has been the subject of several studies (Toniolo et al., 1996), showing that its properties are indistinguishable from those of the natural peptide, including both its three-dimensional structure and biological activity. In this study spectroscopic experiments were made possible by synthesizing a fluorescent analog of trichogin (F10), where a fluorene moiety has been introduced in position 10, by linking Fmc (fluorenyl-9-methylcarbonyl group) to the side chain of an α,γ-diaminobutyric acid (Dab) residue replacing Ile^{10}.

Trichogin is an interesting example for the study of aggregation effects. Due to the high hydrophobicity of its sequence, trichogin is only sparingly soluble in water: already at 50 μM peptide concentration, water solutions of Tric-OMe or F10 become opalescent; therefore, one may expect the formation of aggregates also at the much lower concentrations needed for antibiotic or membrane perturbing activity. Furthermore, ESR spectroscopy studies have shown that this peptide can form aggregates also in apolar solvents such as toluene or chloroform (Milov et al., 2000).

Time-resolved fluorescence spectroscopy is an experimental technique very sensitive to any heterogeneity present in a sample, and therefore it can be very useful for the detection of aggregates or in studies of peptide-membrane association (Stella et al., 2002a). In this report we will show that the membrane activity of trichogin is determined by complex aggregation and partition equilibria: a complete characterization of this behavior will enable us to obtain a new insight into its mechanism of action. A preliminary account of this work has been reported (Stella et al., 2002b).

MATERIALS AND METHODS

Materials

Egg phosphatidylcholine (ePC) and cholesterol were purchased from Avanti Polar Lipids (Alabaster, AL). Carboxyfluorescein and Texas Red (TR)-labeled dextran (average molecular weight 10,000, neutral form) were obtained from Molecular Probes (Eugene, OR). Spectroscopic grade chloroform and methanol (Carlo Erba, Milan, Italy) were used. Polyvinyl alcohol, average molecular weight 22,000, 88% hydrolyzed, and Triton X-100 were purchased from Acros (Geel, Belgium), while Sephacryl S-300 and Sephadex G-50 were purchased from Sigma (St. Louis, MO). Fluoren-9-acetic acid is an Aldrich (St. Louis, MO) product.

Peptide synthesis

Synthesis of peptide F10, Oct-Aib-Gly-Leu-Aib-Gly-Gly-Leu-Aib-Gly-Dab(Fmc)-Lol, was carried out in solution using the fragment condensation approach. Peptide coupling reactions were performed by either the 1-(3-dimethylaminopropyl)-3-ethylcarbodiimide (EDC)/HOBt (1-hydroxy-1,2,3-benzotriazole) (König and Geiger, 1970) or by the EDC/HOAt (7-aza-1-hydroxy-1,2,3-benzotriazole) method (Carpino, 1993). The Fmc group was introduced into the Dab side chain using EDC/HOAt. Details of the synthesis and characterization of peptide F10 were reported by Didonè (2001).

Liposome preparation

Large unilamellar vesicles (LUVs) were prepared by dissolving ePC and cholesterol (1:1 molar ratio) in a chloroform/methanol solution (2:1 v/v). The solvents were evaporated under reduced argon atmosphere until a thin film was formed. Complete evaporation was ensured by applying a rotary vacuum pump for at least 2 h. The film was hydrated with a 20 mM Tris buffer (pH 7.0), containing 140 mM NaCl, whereas for release experiments a 30 mM carboxyfluorescein solution was used. After vigorous stirring and 10 freeze and thaw cycles, the liposome suspension was extruded for 31 times through two stacked polycarbonate membranes with 100 nm pores (Avestin, Ottawa, ON, Canada). Small unilamellar vesicles were prepared by sonication (Auvin-Guette et al., 1992). The unencapsulated fluorescent tracer was separated from the liposomes by gel filtration on a Sephadex G-50 medium column (in the case of carboxyfluorescein) or a Sephacryl S-300 column for dextran. Final phospholipid concentration was determined by the Stewart method (Stewart, 1980). Total concentration (ePC + cholesterol) is reported.

CD and fluorescence spectroscopy

Circular dichroism (CD) spectra were performed with a J-600 Jasco (Tokyo, Japan) instrument. Steady-state fluorescence spectra were measured on a SPEX (Edison, NJ) FluoroMax fluorimeter. Time-resolved experiments were performed on a CD900 single photon counting apparatus by Edinburgh Instruments (Edinburgh, UK). Nanosecond pulsed excitation was obtained with a flash-lamp filled with ultrapure hydrogen (0.3 bar, 30 kHz repetition rate; full width at half-maximum 1.2 ns). Fluorescence intensity decays were acquired until a peak value of 10^4 counts was reached, and analyzed with the software provided by Edinburgh Instruments. Temperature was controlled within $\pm0.1°C$ with a thermostatted cuvette holder. The fluorene chromophore was excited at 265 nm, and time-resolved fluorescence decays were acquired collecting emission at 315 nm, with a bandwidth of 20 nm and a WG305 cutoff filter. Water-membrane partition experiments were performed by using $\lambda_{exc.} = 288$ nm and $\lambda_{em.} = 330$ nm, and correcting intensities for scattering effects according to Ladokhin et al. (2000) using tryptophan as a reference.

To minimize peptide adsorption on cell walls, cuvettes were treated overnight with a 5% (w/w) water solution of polyvinyl alcohol (Barret et al., 2001). Peptide was put into water solutions by adding small aliquots of a methanol solution, so that the concentration of methanol in the final

solution was always below 1%. Controls demonstrate that this amount of methanol does not induce any leakage.

Liposome leakage

Perturbation of membrane permeability was determined by measuring the fractional release of a fluorophore entrapped inside liposomes. In the case of carboxyfluorescein, this quantity can be measured directly by the increase in fluorescence intensity (excitation 490 nm, emission 520 nm) caused by the reduction in self-quenching (Chen and Knutson, 1988). When the entrapped molecule was TR-labeled dextran (0.1 mM concentration), leakage was measured by adding to the outside solution anti-TR antibodies to a 10 μg/mL final concentration. Antibody binding to the fluorophore causes a change in the fluorescence intensity (Sharpe and London, 1999), measured with $\lambda_{exc.} = 592$ nm and $\lambda_{em.} = 604$ nm. In both cases, fractional release (R) was determined by the following formula:

$$R = \frac{F - F_{0\%}}{F_{100\%} - F_{0\%}},$$

where $F_{0\%}$ is the fluorescence intensity before peptide addition, and $F_{100\%}$ is the intensity corresponding to 100% leakage, determined after vesicles were completely disrupted by adding Triton X-100. The release kinetics was recorded with a 0.2 s time step.

Measurements of the intensity of light scattered at 90° were performed in the fluorimeter with both monochromators set at 600 nm.

Aggregation and partition equilibria

Our analysis of peptide aggregation takes into account only two species, namely the monomer and the aggregate, according to the following equilibrium:

$$n\,M \rightleftharpoons M_n, \tag{1}$$

where n is the number of monomers in the aggregate. The aggregation constant is defined as

$$(K_A)^{n-1} = \frac{x_a}{[x_m]^n}, \tag{2}$$

where x_a and x_m are the molar fractions of aggregate and monomer, respectively.

Let us define also the fraction of single peptide chains participating in aggregates (that will be our experimental observable):

$$f_a = \frac{nx_a}{x_p}, \tag{3}$$

where x_p is the total molar fraction of peptide, as given by

$$x_p = x_m + nx_a. \tag{4}$$

If the moles of peptide can be neglected in comparison to the moles of solvent, x_p is given by the ratio between the molar concentrations of peptide and solvent ($C_p/C_{solv.}$).

By combining Eqs. 2, 3, and 4, f_a can be obtained as a function of n, K_A, and x_p:

$$f_a = n(1 - f_a)^n (K_A x_p)^{n-1}. \tag{5}$$

The values of n and K_A can be obtained by fitting experimental aggregation data by a numerical iterative procedure (Fig. 3).

In our case, experimental data indicate that aggregates form both in water and in the membrane phase. Therefore four different peptide species are present in a liposome-containing solution, namely monomer in water, monomer in membrane, aggregate in water, and aggregate in membrane. The fraction of peptide chains participating in each of these four species can be defined by the

following equations (where the concentration of the species in the water or membrane phase is always calculated by using the total volume of the solution):

$$\alpha_{monomer}^{water} = \frac{[M]_{water}}{C_p}; \quad \alpha_{monomer}^{membrane} = \frac{[M]_{membrane}}{C_p};$$

$$\alpha_{aggregate}^{water} = \frac{n[M_n]_{water}}{C_p}; \quad \alpha_{aggregate}^{membrane} = \frac{n'[M_{n'}]_{membrane}}{C_p}, \tag{6}$$

where n and n' are the number of monomers forming the aggregate in water and in the membrane, respectively. These fractions can be determined by time-resolved experiments (Fig. 7); from their values, the aggregated fraction and the total molar fraction of peptide in each phase can be calculated:

$$f_{aggregate}^{water} = \frac{\alpha_{aggregate}^{water}}{\alpha_{monomer}^{water} + \alpha_{aggregate}^{water}}$$

$$x_p^{water} = \left(\alpha_{monomer}^{water} + \alpha_{aggregate}^{water}\right)\frac{C_p}{[W]}$$

$$f_{aggregate}^{membrane} = \frac{\alpha_{aggregate}^{membrane}}{\alpha_{monomer}^{membrane} + \alpha_{aggregate}^{membrane}}$$

$$x_p^{membrane} = \left(\alpha_{monomer}^{membrane} + \alpha_{aggregate}^{membrane}\right)\frac{C_p}{[L]}, \tag{7}$$

where we have assumed that the concentration of peptide in the water or lipid phase is always much lower than total water concentration [W] and lipid concentration [L], respectively. These conditions are always fulfilled under the experimental conditions used in this study.

As the quantities defined in Eqs. 7 describe the aggregation equilibria in the water and membrane phases, separately, they are related by Eq. 5. A fitting of these data allows us to determine the aggregation constant in both phases (Fig. 10).

Monomeric peptides can partition between the water and membrane phases according to the equilibrium described by the following partition constant (White et al., 1998):

$$K_P = \frac{\dfrac{[M]_{membrane}}{[L] + [M]_{membrane}}}{\dfrac{[M]_{water}}{[W] + [M]_{water}}} \simeq \frac{[W][M]_{membrane}}{[L][M]_{water}}. \tag{8}$$

In this case, the fraction of membrane-bound monomer follows a simple Langmuir isotherm as a function of total lipid concentration:

$$f_{membrane-bound\ monomer} = \frac{[M]_{membrane}}{[M]_{total}} = \frac{\dfrac{K_P}{[W]}[L]}{1 + \dfrac{K_P}{[W]}[L]}. \tag{9}$$

This fraction can be calculated from the relative populations of the species (Eqs. 6), determined by time-resolved experiments (Fig. 10), according to the following equation:

$$f_{membrane-bound\ monomer} = \frac{\alpha_{monomer}^{membrane}}{\alpha_{monomer}^{membrane} + \alpha_{monomer}^{water}}. \tag{10}$$

RESULTS

Comparison between Tric-OMe and its fluorescent analog

Absorption and emission spectra of the F10 analog in methanol solution (not shown) are typical of the fluorene

chromophore (Pispisa et al., 2000c). In Fig. 1, the far-ultraviolet (UV) CD spectra of the F10 analog and of Tric-OMe in methanol solution are compared. The similarity of the two spectra suggests that no significant structural perturbation is caused by the introduction of the fluorescent label, and that F10 presents the same structural features observed for the natural peptide (Toniolo et al., 1996). Furthermore, the lack of an induced dichroic contribution by the fluorene moiety, although absorbing strongly in this spectral region, indicates that the fluorophore is not significantly perturbed by the dissymmetric peptide chain.

To assay the membrane permeabilizing activity of the fluorescent analog, the peptide-induced release of a fluorescent marker (carboxyfluorescein) trapped inside liposomes was measured (Fig. 2). Also in this case, the behavior of F10 and Tric-OMe is remarkably similar.

These results demonstrate that the fluorescent label does not perturb the properties of the trichogin analog, and therefore that F10 can be used as a relevant model of the natural peptide.

Peptide aggregation in water

Fig. 3 A illustrates the fluorescence decay of aqueous solutions of F10 as a function of concentration. The decay of the reference compound fluoren-9-acetic acid (Fmc-OH) is well described by a single exponential ($\tau = 5.6 \pm 0.1$ ns $\chi^2 = 1.0$). F10 has a very similar decay at the lowest concentration studied. However, when peptide concentration is increased, a second decay component becomes evident and its relative weight increases. All of the F10 fluorescence decay data can be fitted globally (Beechem et al., 1991) by assuming a double exponential function with lifetimes 5.6 ± 0.1 ns and 0.87 ± 0.08 ns (global $\chi^2 = 1.0$). As the longest component coincides with the lifetime of the reference compound, it can be assigned to the monomeric peptide. The relative weight of the shortest lifetime component is reported in Fig. 3 B: its dependence on peptide concentration is the behavior expected for an aggregation equilibrium (Eq. 5).
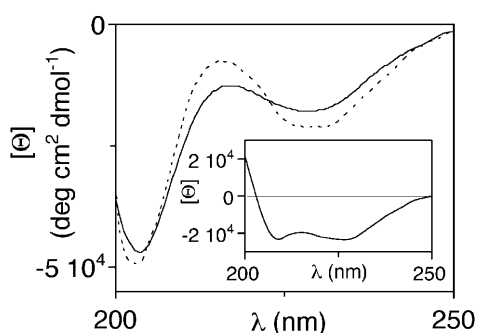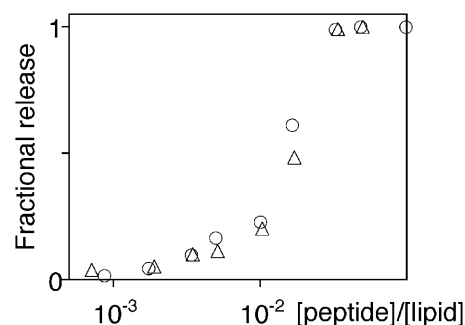

FIGURE 2 Peptide-induced leakage of carboxyfluorescein entrapped inside ePC/cholesterol small unilamellar vesicles (total lipid concentration 60 μM). Triangles, Tric-OMe; circles, F10. Fractional release was determined 20 min after peptide addition.

Therefore, this component can be tentatively assigned to an oligomeric species. Since the same lifetimes are observed at all peptide concentrations, it can be assumed (at least to a first approximation) that only two species (monomer and aggregate) are present in this concentration range. The curve in Fig. 3 B represents a fit of the data based on this model (see Materials and Methods): the resulting parameters are $n = 2.3$ and $K_A^{water} = (3.4 \pm 0.2)10^7$. It must be noted that n represents a Hill-like parameter, because we have postulated the absence of aggregates of varying size. Therefore, n indicates only a lower limit to the maximum number of peptide
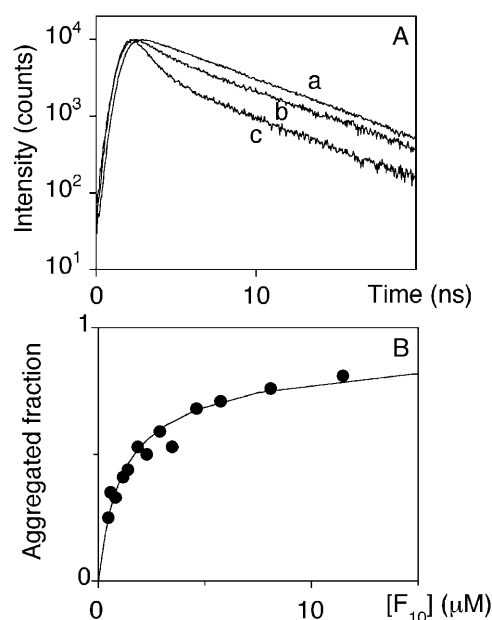

FIGURE 1 Far-UV CD spectra of Tric-OMe (*solid line*) and F10 (*dashed line*) in methanol solution. Solid line, Tric-OMe; broken line, F10. The inset shows the CD of Tric-OMe (97 μM) in a water solution of ePC/cholesterol liposomes (1.0 mM).

FIGURE 3 Time-resolved fluorescence data in water solution. (*A*) Intensity decay curves for Fmc-OH (*a*), F10 (1.9 μM) (*b*), and F10 (11 μM) (*c*). (*B*) Pre-exponential factor associated to the short lifetime component, corresponding to the molar fraction of aggregated peptide, as a function of total peptide concentration. The solid line represents a fit to the data according to an aggregation equilibrium (Eq. 5).

chains participating to the oligomeric species. In any case, our data suggest a relatively small size for the aggregates.

Further experiments have been performed to better characterize the aggregates. Fig. 4 shows the CD spectra of F10 and Tric-OMe in water. The spectrum of the latter peptide exhibits only subtle changes in the position of the peaks, as compared to that obtained in methanol (Fig. 1), where aggregation does not occur in the concentration range studied. By contrast, the CD of F10 in water differs significantly because of an induced dichroism of fluorene, thereby confirming a perturbation of this chromophore in the aggregates. In principle, this could be due either to probe-probe or to probe-peptide interactions. We have measured the fluorescence decay in water at a fixed total peptide concentration (4.6 μM), varying the relative amount of labeled and unlabeled peptide (F10 and Tric-OMe) within the range of 1:3 and 3:1 ratios. Within the experimental error, the time-resolved fluorescence curves do not change, thereby indicating that lifetime quenching is not caused by interprobe interactions and also that Tric-OMe has an aggregation behavior similar to that of the labeled peptide.

Membrane-water partition

The membrane-water partition of the F10 analog was determined by measuring the change in fluorescence intensity caused by the addition of increasing concentrations of liposomes (White et al., 1998). Fig. 5 shows the partition curves measured at three different peptide concentrations (1.1, 11, and 30 μM): as the peptide concentration increases, association with the phospholipid bilayer is progressively less favored. This dependence on peptide concentration shows that peptide-membrane association cannot be described by a partition equilibrium of a single species (Eq. 9), and strongly suggests the occurrence of aggregation phenomena (Rizzo et al., 1987).

To get a better characterization of the peptide behavior, time-resolved fluorescence measurements of F10 (at different peptide concentrations) in the presence of liposomes at a phospholipid concentration of 0.2 and 2.0 mM were
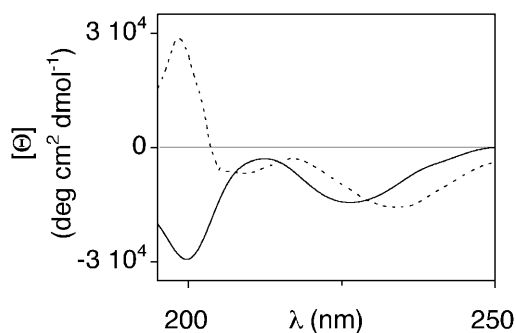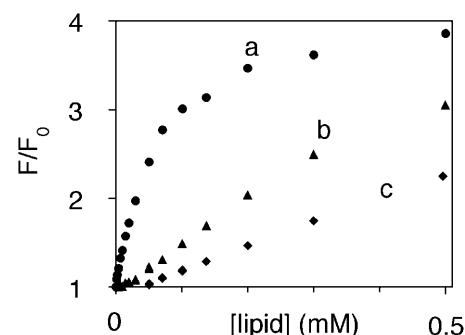
FIGURE 5 Membrane-water partition curves for F10 detected by the fluorescence intensity (F), normalized by the intensity in the absence of liposomes (F_0). Peptide concentration: 1.1 μM (*a*), 11 μM (*b*), and 30 μM (*c*). ePC/Chol LUVs were used.

performed. On the basis of the partition curves, the membrane-bound peptide is always in equilibrium with the water phase. Therefore, we expect a very complex fluorescence decay behavior, where the monomeric and aggregated peptides in the water phase contribute to the overall fluorescence. However, the lifetimes of these components were preliminary determined in the absence of liposomes (Fig. 3). The simplest possible decay model is a triple exponential function, with two lifetimes fixed to the values measured in water and the third component corresponding to the membrane-bound peptide (Fig. 6). Unfortunately, this fit is not
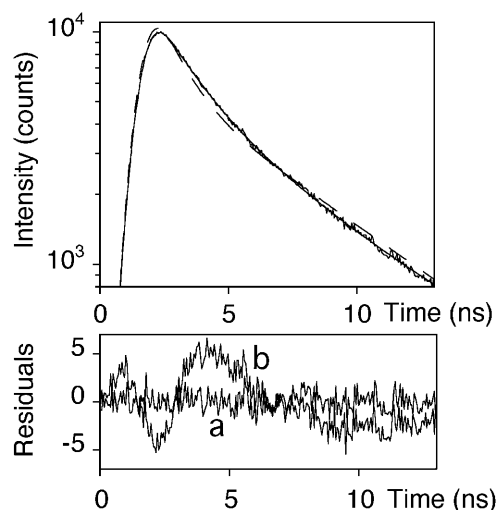
FIGURE 6 (*Upper panel*) Fluorescence intensity decay of F10 (50 μM) in the presence of ePC/cholesterol liposomes (2 mM). The dashed line represents a fit to this decay with a triple exponential function, with two lifetimes fixed to the values observed in the absence of liposomes (Fig. 3), and the remaining one left as a free fitting parameter. The solid line is a fit with the sum of four exponential functions, with two lifetimes fixed to the values observed in the absence of liposomes, and the other two used as global parameters in a global fit of the fluorescence decay observed at 10 different peptide concentrations (Fig. 7). (*Lower panel*) Residuals of the fits reported in the upper panel, showing the superiority of the four exponential global fit (*curve a*) as compared to the triple exponential fit (*curve b*).

FIGURE 4 Far-UV CD spectra of Tric-OMe (*solid line*) and F10 (*dashed line*) in water solution at 6 μM peptide concentration.

adequate to describe the experimental decays: a global χ^2 value of 4.6 is obtained if the third lifetime is assumed independent of peptide concentration, and this value decreases only to 2.3 if the third lifetime is allowed to vary. In the latter case, the additional lifetime exhibits a random behavior as a function of peptide concentration. These results show that a single component is not sufficient to describe the membrane-bound peptide fraction. To take this conclusion into account, the next simplest assumption is that at least two different species do occur also in the membrane phase. Therefore, a model with two lifetime components, in addition to those describing the water phase, was tested, assuming these additional lifetimes independent of peptide concentration (i.e., "global" parameters). The recovered global χ^2 is 0.95, and this fit is satisfactory also as judged from the distribution of residuals (Fig. 6). The two lifetimes associated to the membrane-bound species are 2.2 ± 0.2 ns and 7.0 ± 0.2 ns. The molar fractions related to each lifetime component in the presence of 2 mM lipid concentration are reported in Fig. 7; each of the four components shows a clear and distinctive trend as a function of peptide concentration. A detailed analysis, confirming the soundness of this model in describing the time-resolved fluorescence data, will be presented below, in the "Discussion" section.

To determine whether the two membrane-bound species play a different role in bilayer perturbation, the behavior of peptide-induced membrane permeability as a function of total peptide concentration was compared to the variation of the concentration of the different species in the membrane phase. A strong correlation is found only when the concentration of the membrane-bound species associated to the 2.2 ns lifetime component is considered (Fig. 8). On the other hand, the total peptide concentration in the membrane phase shows a different behavior, thereby suggesting that only one of the two membrane-associated species is active in perturbing the bilayer permeability.

CD measurements in the presence of liposomes (Fig. 1, *inset*) show that a distinct conformational transition is
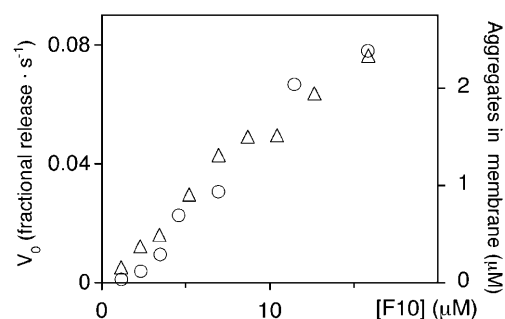
FIGURE 8 Comparison between the behavior of membrane-perturbing activity (initial rate of liposome content release: *circles, left scale*) and of the concentration of membrane-bound aggregates (*triangles, right scale*), as a function of total peptide concentration, in the presence of ePC/cholesterol LUVs (0.2 mM). The concentration of membrane aggregates is derived from the relative population associated to the 2.2 ns lifetime component (see "Discussion").

induced by membrane binding, since the spectral shape of Tric-OMe resembles very closely that of a canonical α-helix.

Release experiments

Further experiments were performed to obtain a more direct evidence on the mechanism of membrane perturbation. If the release of liposome contents were caused by disruption of the vesicles by a "detergent-like" mechanism, then a drastic decrease in particle size would be expected as a consequence of liposome micellization. This effect can be detected by the intensity of the light scattered by the vesicle suspension (Jones and Cossins, 1990). For instance, when a detergent such as Triton is added, the intensity of light scattering decreases by a factor of 15, as a consequence of liposome micellization. On the other hand, when F10 or Tric-OMe is added at concentrations that cause an almost complete release of the liposome content, only changes in light scattering below 10% are observed, thus suggesting that vesicle size is not significantly perturbed.

As a further characterization of the peptide-induced permeability, leakage of carboxyfluorescein (molecular weight 376) was compared to the release of Texas Red-labeled dextran (average molecular weight 10,000). As shown in Fig. 9, the larger molecule is released to a much lower extent at all peptide concentrations examined.

DISCUSSION

Heterogeneity in the membrane phase

Our data show that trichogin GA IV has a strong tendency to form oligomers in water (aggregation is almost complete already at 10 μM peptide concentration). Furthermore, time-resolved experiments in the presence of liposomes indicated that a single lifetime component is not sufficient to describe the membrane-bound peptide fraction, a finding deserving
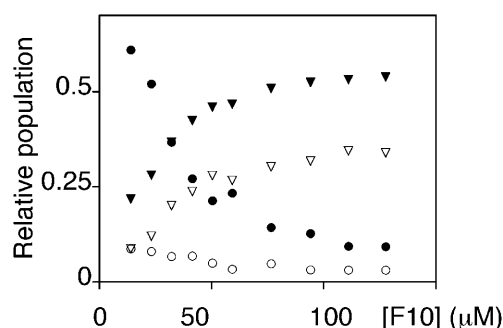

FIGURE 7 Pre-exponential factors determined from time-resolved fluorescence data for F10 in the presence of ePC/cholesterol LUVs (2 mM), corresponding to the following lifetimes: 0.87 ns (*open triangles*), 2.2 ns (*solid triangles*), 5.6 ns (*open circles*), and 7.0 ns (*solid circles*).
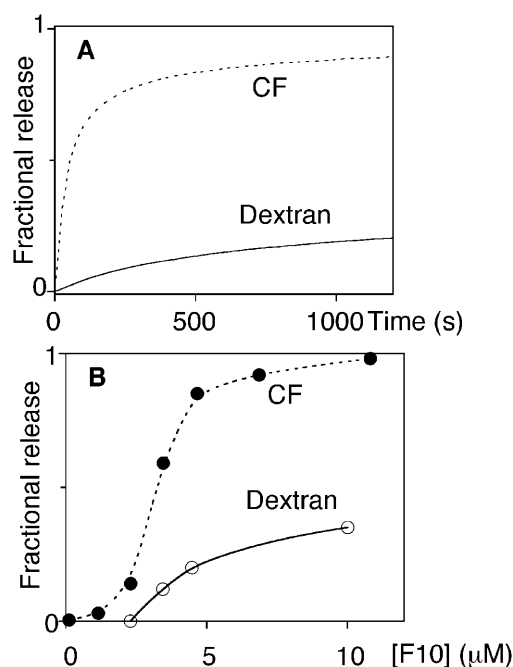
FIGURE 9 Comparison of carboxyfluorescein and Texas Red-labeled dextran (<molecular weight> = 10,000) release from liposomes (0.2 mM), induced by F10 addition. (*A*) Kinetics of release; 4.5 μM F10 was added at time 0. (*B*) Peptide concentration dependence of the fractional release 20 min after peptide addition. The continuous curves in panel *B* are just a guide to the eye.

SCHEME I

a few comments. In principle, a multi-exponential decay could be due to different factors, i.e., slow relaxation of the membrane environment, ground-state heterogeneity resulting from different environments around the fluorophore, or the occurrence of different states of the peptide (Ladokhin and White, 2001a). The observation that the fluorescence decay of the membrane-bound peptide fraction is strongly dependent on peptide concentration definitely rules out conformational heterogeneity and solvent relaxation as the main reasons for the multi-exponential decay observed. This latter hypothesis is very unlikely also because the emission spectrum of fluorene is almost completely insensitive to solvent polarity. On the other hand, the peptide concentration dependence of the multi-exponential fluorescence decay strongly suggests that the heterogeneity arises from different aggregation states in the membrane phase, although the possibility of a concentration-induced change in orientation (Huang, 2000) cannot be completely ruled out. Our model is presented in Scheme I: in both the water and membrane phases, the peptide is in equilibrium between a monomeric and an aggregated state. Furthermore, monomers in the two phases are related by a partition equilibrium. In principle, also the aggregates could associate to or dissociate from the lipid bilayer. However, the aggregates in the two phases have very likely a significantly different structure and/or size, as due to the diverging physico-chemical environments. As a result, the aggregated species in the two phases cannot be
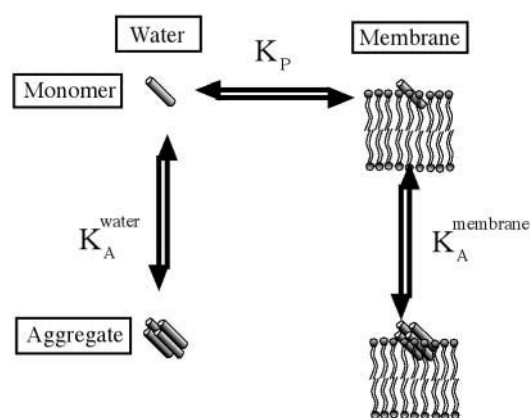
related by a simple partition equilibrium. All the same, the three equilibria described above (aggregation in the two phases and partition of monomers) are sufficient to define the relative concentration of the four species (monomer and aggregate in the two phases). It is reasonable to assume that these four different species would correspond to the four lifetime components observed in the time-resolved fluorescence experiments. Furthermore, the model reported in Scheme I, with its interconnected equilibria, predicts a dependence of peptide-membrane association on total peptide concentration, as observed for our system in Fig. 5 (Rizzo et al., 1987).

The weight of the longest lifetime observed in the membrane phase (7.0 $\pm$ 0.2 ns) decreases with increasing peptide concentration. Therefore, according to our aforementioned interpretation, this lifetime corresponds to the membrane-bound monomer, whereas the other component (2.2 $\pm$ 0.2 ns) may be assigned to the oligomer. This hypothesis is supported by the finding that the aggregated form is substantially quenched with respect to the monomer, as already observed in water. Furthermore, both species have a significantly longer lifetime in the membrane phase than in water, as expected from the increase in fluorescence intensity caused by membrane binding. With this association between fluorescence lifetimes and peptide species, we can now test if the data reported in Fig. 7 follow the model reported in Scheme I. The easiest way is by analyzing each of the three proposed equilibria separately.

Fig. 10 *A* shows the water-membrane partition equilibrium of the monomer. The fraction of membrane-associated monomer has been calculated from the data of Fig. 7 according to Eq. 10. As expected for a simple partition equilibrium, this fraction does not depend on peptide concentration (Eq. 9). From its value, a partition constant $K_P = (1.3 \pm 0.3)10^5$ is obtained.

Fig. 10, *B* and *C*, describe the aggregation equilibria in the water and membrane phases, respectively. The fraction of peptide chains giving rise to aggregates is plotted as a function of the molar fraction of peptide in each phase.
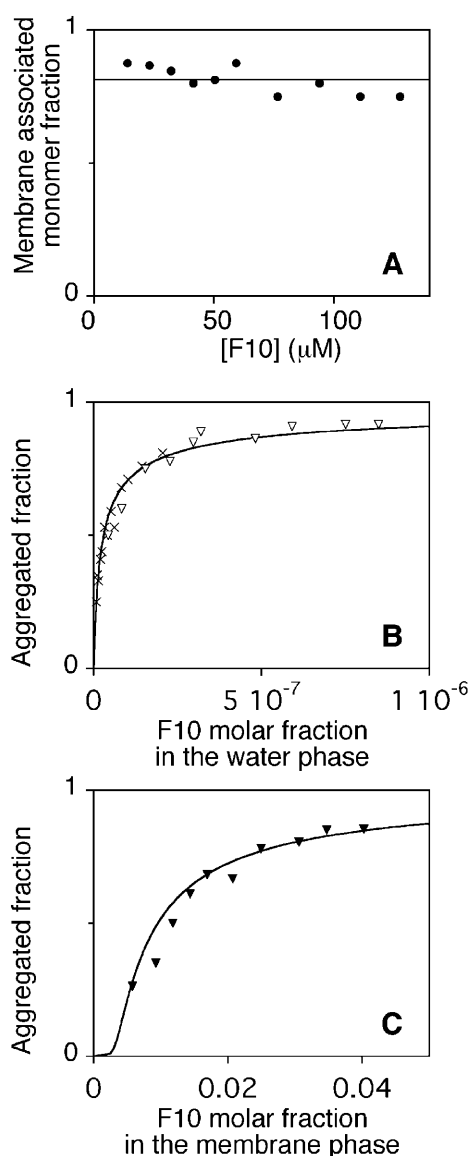
FIGURE 10   (*A*) Water-membrane partition equilibria of monomeric F10 in the presence of ePC/cholesterol liposomes (2mM). (*B*) Aggregation equilibrium of F10 in water (*triangles*), derived from the time-resolved data in the presence of membranes (Fig. 7) by using Eqs. 7. For comparison, the aggregation data measured directly in water (Fig. 3) are also shown (*crosses*), together with their fit to Eq. 5. (*C*) Aggregation equilibrium of F10 in the membrane phase, obtained from the data of Fig. 7 by using Eqs. 7. The continuous curve is a fit of these data to Eq. 5.

These quantities have been calculated from the data reported in Fig. 7 according to Eqs. 7. The first observation is that the data describing aggregation in water obtained by this analysis are exactly coincident with the measurements of peptide aggregation performed in the absence of membranes (Fig. 3), a finding strongly supporting the proposed interpretation. On the other hand, the curve describing the aggregation equilibrium in the membrane (Fig. 10 *C*) shows that aggregation in this phase is much less favored as

compared to water and exhibits a marked sigmoidal shape. If these data are treated according to Eq. 5, the values of $n = 8.0$ and $K_A^{membrane} = 154 \pm 8$ are obtained (continuous line in Fig. 10 *C*), showing that aggregates in the membrane phase are larger than in water.

In summary, the good agreement between the experimental behavior described in Fig. 10 and the predictions of the aggregation and partition equilibria of our model strongly supports the view that the heterogeneity observed for the peptide fluorescence decay in the membrane phase is primarily due to the formation of aggregates. It is also worth mentioning that preliminary results on fluorescence energy-transfer between trichogin analogs labeled with different fluorophores (data not shown) show that transfer efficiency in the membrane phase is much higher than that expected for a random dispersion of the peptides, thus confirming the presence of aggregates (Strahilevitz et al., 1994).

Finally, it is worth noting that the behavior observed here for trichogin shows several similarities with that reported for alamethicin, the best-studied member of the peptaibol family. This peptide forms aggregates both in water and in the membrane phases (Rizzo et al., 1987), its aggregation constant in the membrane ($K_A^{membrane}$[alamethicin] ≈ 700) being of the same order of magnitude as that observed here for trichogin. On the other hand, aggregation in water for alamethicin is much less favored than that of trichogin, probably because of the higher hydrophobicity of the latter peptide. This is also the reason why the partition constant between water and membrane for monomeric alamethicin (K_P[alamethicin] $\approx 3 \ 10^4$) is lower than that of trichogin.

Mechanism of membrane permeabilization

Our data show that trichogin-induced leakage is not due to liposome lysis and is size-selective: carboxyfluorescein, with a size of ~ 1 nm, is easily released, whereas leakage of dextran molecules, with a hydrodynamic diameter of 4 nm (Rex, 1996), is minor and very likely due to the polydispersity of the polysaccharide (Fig. 9). Therefore, formation of pores seems to be responsible for the increase in membrane permeability, and membrane disruption by a detergent-like mechanism (Ladokhin and White, 2001b) can be ruled out, at least within the concentration range investigated. According to the correlation shown in Fig. 8, only one of the membrane-bound species, namely the aggregated form, is active in causing a perturbation of the membrane permeability, suggesting that pores are formed by the aggregated peptide. Interestingly, Kropacheva and Raap (2002) have recently shown that trichogin is able to enhance the ion conduction of membranes in a selective and potential-dependent manner. This behavior is similar to that of peptides such as zervamicin or alamethicin, which are thought to form channels by a ''barrel-stave'' mechanism. However, these authors ruled out a similar model in the case of trichogin, mainly because a peptide concentration ~ 200

times larger than that of zervamicin is needed by trichogin to cause ion leakage. A direct comparison between the membrane association curves of zervamicin and trichogin shows that the affinities of the two peptides for phospholipid bilayers differ approximately by two orders of magnitude. Furthermore, our data indicate that only a fraction of membrane-bound trichogin forms aggregates and causes leakage. Taken together, these results suggest that the discrepancy observed in peptide activity between the two peptides may simply arise from a different partition behavior and not from a different mechanism of action.

Partition, aggregation, and activity

Lipidation of bioactive peptides has been proposed as a way to increase their membrane binding, biological activity, and bioavailability (Pedersen et al., 2001; Avrahami and Shai, 2002; Silvius, 2002). Our results suggest that several factors must be taken into account in these processes, because the introduction of a long acyl chain may lead either to an increased membrane affinity or to the formation of aggregates in water, which causes a reduced partition into the membrane phase. The occurrence of this phenomenon is supported by studies on trichogin analogs with acyl chains of different length (Toniolo et al., 1996), which showed that the membrane-perturbing activity increases up to a chain length of 10 carbon atoms, whereas a further elongation of the aliphatic chain causes a lower activity.

More generally, our results show that the ratio between peptide and lipid concentration is not the only parameter to be considered when discussing peptide activity. For instance, the dependence of trichogin-induced leakage on peptide/lipid ratio is different when experiments are performed at 60 μM (Fig. 2) or 600 μM lipid concentration (Toniolo et al., 1996). This result is easily understood on the basis of the partition data presented here, as due to a difference in the fraction of membrane-bound active peptide.

CONCLUDING REMARKS

Three major conclusions can be drawn from the data set reported here. First, trichogin GA IV forms aggregates both in water and in the membrane phase. Second, membrane permeability is caused by these aggregates only. Third, within the concentration range explored, trichogin induces membrane leakage by forming pores rather than by a detergent-like mechanism. All aggregation and partition equilibria observed in our experiments concur to determine the dependence of trichogin activity on peptide concentration. Since a similar behavior is very likely shared by many other antibiotic peptides, our results suggest that aggregation and water-membrane partition equilibria need to be fully characterized before comparing the biological activity and the molecular mechanism of action of different peptides.

REFERENCES

Auvin-Guette, C., S. Rebufatt, Y. Prigent, and B. Bodo. 1992. Trichogin A IV, an 11-residue lipopeptaibol from *Trichoderma longibrachiatum*. *J. Am. Chem. Soc.* 114:2170–2174.

Avrahami, D., and Y. Shai. 2002. Conjugation of a magainin analogue with lipophilic acids controls hydrophobicity, solution assembly, and cell selectivity. *Biochemistry*. 41:2254–2263.

Barret, D. A., M. S. Hartshorne, M. A. Hussain, P. N. Shaw, and M. C. Davies. 2001. Resistance to nonspecific protein adsorption by poly(vinyl alcohol) thin films adsorbed to a poly(styrene) support matrix studied using surface plasmon resonance. *Anal. Chem.* 73:5232–5239.

Beechem, J. M., E. Gratton, M. Ameloot, J. R. Knutson, and L. Brand. 1991. The global analysis of fluorescence intensity and anisotropy decay data: second generation theory and programs. *In* Topics in Fluorescence Spectroscopy, Vol. 2: Principles. J. R. Lakowicz, editor. Plenum Press, New York. 241–305.

Carpino, L. 1993. 1-Hydroxy-7-azo-benzotriazole. An efficient peptide coupling additive. *J. Am. Chem. Soc.* 115:4397–4398.

Chen, F. Y., M. T. Lee, and H. W. Huang. 2002. Sigmoidal concentration dependence of antimicrobial peptide activities: a case study on alamethicin. *Biophys. J.* 82:908–914.

Chen, R. F., and J. R. Knutson. 1988. Mechanism of fluorescence concentration quenching of carboxyfluorescein in liposomes: energy transfer to nonfluorescent dimers. *Anal. Biochem.* 172:61–77.

Didonè, M. 2001. Trichogin analogs for photophysical studies in membranes. Chemistry MSc thesis. University of Padua, Padua, Italy.

Epand, R. M., and H. J. Vogel. 1999. Diversity of antimicrobial peptides and their mechanisms of action. *Biochim. Biophys. Acta*. 1462:11–28.

Huang, H. W. 2000. Action of antimicrobial peptides: two-state model. *Biochemistry*. 39:8347–8352.

Jones, G. R., and A. R. Cossins. 1990. Physical methods of study. *In* Liposomes: A Practical Approach. R. R. C. New, editor. Oxford University Press, Oxford. 183–220.

Karle, I. L., and P. Balaram. 1990. Structural characteristics of alpha-helical peptide molecules containing Aib residues. *Biochemistry*. 29:6747–6756.

König, W., and R. Geiger. 1970. A new method for synthesis of peptides: activation of the carboxyl group with dicyclohexylcarbodiimide using 1-hydroxybenzotriazoles as additives. *Chem. Ber*. 103:788–798.

Kropacheva, T. N., and J. Raap. 2002. Ion transport across a phospholipid membrane mediated by the peptide trichogin GA IV. *Biochim. Biophys. Acta*. 1567:193–203.

Ladokhin, A. S., S. Jayasinghe, and S. H. White. 2000. How to measure and analyze tryptophan fluorescence in membranes properly, and why bother? *Anal. Biochem.* 285:235–245.

Ladokhin, A. S., and S. H. White. 2001a. Alphas and taus of tryptophan fluorescence in membranes. *Biophys. J.* 81:1825–1827.

Ladokhin, A. S., and S. H. White. 2001b. 'Detergent-like' permeabilization of anionic lipid vesicles by melittin. *Biochim. Biophys. Acta*. 1514: 253–260.

Matsuzaki, K. 2001. Molecular mechanisms of membrane perturbation by antimicrobial peptides. *In* Development of Novel Antimicrobial Agents: Emerging Strategies. K. Lohner, editor. Horizon Scientific Press, Wymondham, UK. 167–181.

Milov, A. D., Y. D. Tsvetkov, F. Formaggio, M. Crisma, C. Toniolo, and J. Raap. 2000. Self-assembling properties of membrane-modifying peptides studied by PELDOR and CW-ESR spectroscopies. *J. Am. Chem. Soc.* 122:3843–3848.

Pedersen, T. B., M. C. Sabra, S. Frokjaer, O. G. Mouritsen, and K. Jørgensen. 2001. Association of acylated cationic decapeptides with dipalmitoylphosphatidylserine-dipalmitoylphosphatidylcholine lipid membranes. *Chem. Phys. Lipids*. 113:83–95.

Pispisa, B., L. Stella, M. Venanzi, A. Palleschi, F. Marchiori, A. Polese, and C. Toniolo. 2000a. A spectroscopic and molecular mechanics investigation on a series of Aib-based linear peptides and a peptide

template, both containing tryptophan and a nitroxide derivatives as probes. *Biopolymers.* 53:169–181.

Pispisa, B., L. Stella, M. Venanzi, A. Palleschi, C. Viappiani, A. Polese, F. Formaggio, and C. Toniolo. 2000b. Quenching mechanisms in bichromophoric, 3_{10}-helical Aib-based peptides, modulated by chain-length dependent topologies. *Macromolecules.* 33:906–915.

Pispisa, B., C. Mazzuca, A. Palleschi, L. Stella, M. Venanzi, F. Formaggio, A. Polese, and C. Toniolo. 2000c. Structural features of linear (αMe)Val-based peptides in solution by photophysical and theoretical conformational studies. *Biopolymers.* 55:425–435.

Rex, S. 1996. Pore formation induced by the peptide melittin in different lipid vesicle membranes. *Biophys. Chem.* 58:75–85.

Rizzo, V., S. Stankowski, and G. Schwarz. 1987. Alamethicin incorporation in lipid bilayers: a thermodynamic study. *Biochemistry.* 26:2751–2759.

Shai, Y. 2002. Mode of action of membrane active antimicrobial peptides. *Biopolymers.* 66:236–248.

Sharpe, J. C., and E. London. 1999. Diphtheria toxin forms pores of different sizes depending on its concentration in membranes: probable relationship to oligomerization. *J. Membr. Biol.* 171:209–221.

Silvius, J. R. 2002. Lipidated peptides as tools for understanding the membrane interactions of lipid-modified proteins. *In* Peptide-Lipid Interactions. S. A. Simon and T. J. McIntosh, editors. Academic Press, London. 371–395.

Stella, L., M. Venanzi, M. Carafa, E. Maccaroni, M. E. Straccamore, G. Zanotti, A. Palleschi, and B. Pispisa. 2002a. Structural features of model glycopeptides in solution and in membrane phase: a spectroscopic and molecular mechanics investigation. *Biopolymers.* 64:44–56.

Stella, L., C. Mazzuca, A. Palleschi, M. Venanzi, F. Formaggio, C. Toniolo, L. Moroder, and B. Pispisa. 2002b. Mechanism of membrane.-permeabilization by the lipopeptaibol trichogin GA IV and its fluorescent analogues. *In* Peptides 2002. E. Benedetti and C. Pedone, editors. Edizioni Ziino, Naples. 894–895.

Stewart, J. C. M. 1980. Colorimetric determination of phospholipids with ammonium ferrothiocyanate. *Anal. Biochem.* 104:10–14.

Strahilevitz, J., A. Mor, P. Nicolas, and Y. Shai. 1994. Spectrum of antimicrobial activity and assembly of dermaseptin-b and its precursor form in phospholipid membranes. *Biochemistry.* 33:10951–10960.

Toniolo, C., M. Crisma, F. Formaggio, C. Peggion, R. F. Epand, and R. M. Epand. 2001. Lipopeptaibols, a novel family of membrane active, antimicrobial peptides. *Cell. Mol. Life Sci.* 58:1179–1188.

Toniolo, C., M. Crisma, F. Formaggio, C. Peggion, V. Monaco, C. Goulard, S. Rebuffat, and B. Bodo. 1996. Effect of N^{α}-acyl chain length on the membrane-modifying properties of synthetic analogs of the lipopeptaibol trichogin GA IV. *J. Am. Chem. Soc.* 118:4952–4958.

Toniolo, C., C. Peggion, M. Crisma, F. Formaggio, X. Shui, and D. S. Eggleston. 1994. Structure determination of racemic trichogin A IV using centrosymmetric crystals. *Nat. Struct. Biol.* 1:908–914.

White, S. H., W. C. Wimley, A. S. Ladokhin, and K. Hristova. 1998. Protein folding in membranes: determining energetics of peptide-bilayer interactions. *Methods Enzymol.* 295:62–87.

Yang, L., T. A. Harroun, T. M. Weiss, L. Ding, and H. W. Huang. 2001. Barrel stave or toroidal model? A case study on melittin pores. *Biophys. J.* 81:1475–1485.

Zasloff, M. 2002. Antimicrobial peptides of multicellular organisms. *Nature.* 415:389–395.